Bmx Tyrosine Kinase Transgene Induces Skin Hyperplasia, Inflammatory Angiogenesis, and Accelerated Wound Healing

Karri Paavonen,* Niklas Ekman,* Maria Wirzenius,* Iiro Rajantie,*
Matti Poutanen,† and Kari Alitalo,*‡

*Molecular/Cancer Biology Laboratory and Ludwig Institute for Cancer Research, Haartman Institute
and Biomedicum Helsinki, University of Helsinki and Helsinki University Central Hospital, Helsinki
FIN-00014, Finland; and †Department of Physiology, Institute of Biomedicine, University of Turku,
Turku FIN-20014, Finland

The *Bmx* gene, a member of the Tec family of nonreceptor protein tyrosine kinases, is expressed in arterial endothelium and in certain hematopoietic and epithelial cells. Previous in vitro studies have implicated Bmx signaling in cell migration and survival and suggested that it contributes to the progression of prostate carcinomas. However, the function of Bmx in normal tissues in vivo is unknown. We show here that Bmx expression is induced in skin keratinocytes during wound healing. To analyze the role of Bmx in epidermal keratinocytes in vivo, we generated transgenic mice overexpressing Bmx in the skin. We show that Bmx overexpression accelerates keratinocyte proliferation and wound reepithelialization. Bmx expression also induces chronic inflammation and angiogenesis in the skin, and gene expression profiling suggests that this occurs via cytokine-mediated recruitment of inflammatory cells. Our studies provide the first data on Bmx function in vivo and form the basis of evaluation of its role in epithelial neoplasia.

INTRODUCTION

Protein tyrosine kinases (PTKs) are involved in the regulation of growth and differentiation of virtually all cell types. The Bmx (B̲one M̲arrow tyrosine kinase gene in chromosome X̲) PTK (Tamagnone *et al.,* 1994), also named Etk for epithelial and endothelial tyrosine kinase (Robinson *et al.,* 1996), is a member of the Tec family of intracellular PTKs. In addition to the *Bmx* gene, this family includes four other closely related genes, the founder member *Tec* as well as *Btk, Itk/Tsk,* and *Txk/Rlk.* The Tec family proteins share a characteristic domain structure with a pleckstrin homology (PH) domain in the amino-terminal part, followed by a Tec homology (TH) domain, src homology 3 (SH3) and 2 (SH2) domains, and a carboxyl-terminal tyrosine kinase domain (Mano, 1999; Qiu and Kung, 2000; Smith *et al.,* 2001).

Mice lacking one or two Tec family members have been generated (Smith *et al.,* 2001). Mice with a deficiency of *Bmx* (Rajantie *et al.,* 2001), *Tec* (Ellmeier *et al.,* 2000), or *Txk* (Schaeffer *et al.,* 1999), do not show any major phenotypic alterations. *Itk,* however, is required for proper T-cell development and activation (Liao and Littman, 1995), and overexpression of Txk in T cells partially rescues Itk deficiency (Sommers *et al.,* 1999). In vivo, the most extensively studied family member so far is *Btk.* This is largely due to the immunodeficiency syndromes that are associated with naturally occurring mutations in the *Btk* gene, X-linked agam-

maglobulinemia (XLA) in humans and x-linked immunodeficiency (xid) in mice (Satterthwaite and Witte, 2000). XLA is characterized by a block in the differentiation of pro-B cells to pre-B cells, leading to a decreased number of B-lymphocytes and an almost total lack of antibody-producing plasma cells. Mice with defects in *Btk* show a similar, but milder phenotype when compared with XLA (Fruman *et al.,* 2000; Satterthwaite and Witte, 2000). Interestingly, when the Tec kinase was overexpressed under the β-actin promoter in transgenic mice, no obvious phenotype could be detected (Honda *et al.,* 1995).

Like the other members of the Tec family, Bmx is expressed in a subset of hematopoietic cells (Kaukonen *et al.,* 1996; Weil *et al.,* 1997). In cultured mouse myeloid progenitor cells, Bmx regulated granulocyte-colony stimulating factor (G-CSF)-mediated granulocytic differentiation (Ekman *et al.,* 2000). In addition, Bmx expression was found in certain nonhematopoietic cells. Using *LacZ* knock-in mice, we demonstrated *Bmx* expression in arterial endothelial cells, in the endocardium, and in a few specific epithelial cells, namely the basal epidermal cells of the tongue and few specialized epithelial cells of the thymus (Rajantie *et al.,* 2001). The function of Bmx in these cells nevertheless remains unclear because the mice deficient of the *Bmx* gene have not shown any phenotypic alterations (Rajantie *et al.,* 2001).

In this study, we have addressed the epithelial function of Bmx in vivo. Although, in normal skin, the *Bmx* gene was expressed only in the arterial endothelium, we found that the gene was strongly up-regulated in keratinocytes during wound healing. To assess the function of Bmx in these cells, we generated transgenic mice overexpressing Bmx in the basal skin keratinocytes. The epithelial Bmx transgene induced a skin phenotype characterized by increased keratin-

ocyte proliferation, inflammatory cell recruitment, and strong dermal angiogenesis. Furthermore, these mice showed an accelerated skin wound healing.

MATERIALS AND METHODS

Transgenic Mice

The cDNA encoding full-length Bmx (accession no. X83107) fused to a C-terminal hemagglutinin (HA) epitope was cloned into a human keratin 14 (K14) promoter expression cassette (a kind gift from Dr. E. Fuchs; Vassar *et al.*, 1989) and injected into fertilized FVB/NIH mouse oocytes. The mice were genotyped using PCR of tail DNA. Amplification of the genomic DNA was carried out using Dynazyme polymerase (Finnzymes Oy, Espoo, Finland) in a total volume of 20 μl with the following conditions: denaturation at 94°C for 30 s, annealing at 53°C for 40 s, and extension at 72°C for 40 s, 28 cycles. The expected PCR product was 354 base pairs with the primers 5′-AATCAGAT-GTGTGGAGAAAG-3′ and 5′-ACTGCCCGAGGTATCTTCA-3′. From 15 independent transgene expressing mouse lines, three lines with high expression of the Bmx mRNA were studied in detail. All animal experiments were approved by the Provincial State Office of Southern Finland.

Wound Experiments

Eight- to 10-week-old mice were anesthetized with ketamine hydrochloride (HCl; 50 mg/kg sc) and xylazine HCl (10 mg/kg sc). The backs of the mice were shaved and the skin was disinfected by swabbing with ethanol. Wounds traversing the skin were made on both sides of the back with a 5-mm punch biopsy tool (Fray Products Corp., Buffalo, NY). Wounds were allowed to heal for 0–21 days after which the mice were sacrificed with carbon dioxide and/or cervical dislocation, and the wounds were collected. Infected wounds were discarded. Samples were fixed in neutral formalin or 4% paraformaldehyde and dehydrated and embedded in paraffin. Hematoxylin and eosin (H&E)-stained sections of the wound sections were photographed and analyzed with an Olympus AX70 microscope (Olympus Europa Gmbh, Hamburg, Germany) and Macintosh computer (Apple Computer, Inc, Cupertino, CA), using the NIH Image program (developed at the U.S. National Institutes of Health and available on the Internet at http://rsb.info.nih.gov/nih-image/). The remaining wound area was quantified by measuring the distance between the migrating epidermal edges and comparing it with the original wound width, i.e., the distance between the edges of the m. panniculus carnosus layer. In wound experiments 3–5 mice (ca. 12–20 wounds) were used for each time point analyzed in each mouse subgroup.

Tumor Implantation

One million T241 fibrosarcoma cells (Gutierrez *et al.*, 2000) in 20 μl of phosphate-buffered saline (PBS) were injected subcutaneously into mice. After 12 days, the mice were sacrificed and the tumors were fixed in PFA, dehydrated, embedded in paraffin and analyzed by immunohistochemistry or β-galactosidase staining as previously reported (Rajantie *et al.,* 2001).

Immunoprecipitation and Western Blotting

For detection of transgene expression by immunoblotting, frozen tissue samples were homogenized and lysed in radioimmunoprecipitation assay (RIPA) buffer supplemented with aprotinin, leupeptin, phenylmethylsulfonyl fluoride (PMSF), and sodium vanadate. Immunoprecipitations were carried out from equal lysate aliquots (1.5 mg total protein) by incubation with mouse monoclonal antibodies against Bmx (BD Biosciences/PharMingen, San Diego, CA) for 2 h, followed by incubation with protein G-sepharose (Amersham Pharmacia Biotech, Piscataway, NJ) for 1 h. The immunoprecipitates were washed and eluted into Laemmli sample buffer. Alternatively for cultured MMC-E epithelial cells, cells were washed with PBS and lysed in boiling lysis buffer (2.5% SDS in 0.5 M Tris-HCl [pH 6.8]). Lysates were sonicated and cleared by centrifugation and protein concentrations were determined using a Bio-Rad DC assay (Bio-Rad Laboratories, Hercules, CA) according to the manufacturer's protocol. The proteins (45 μg) were eluted into Laemmli sample buffer. Tissue and cell culture elutes were fractioned in a 7.5% SDS-PAGE gel under reducing conditions and transferred to a nitrocellulose membrane. The proteins were detected using either monoclonal mouse anti-HA antibodies (Covance Research Products, Princeton, NJ) or rabbit polyclonal antibodies raised against a GST fusion protein containing residues 207–267 of human Bmx followed by HRP-conjugated anti-mouse or anti-rabbit secondary antibodies (DakoCytomation Denmark A/S, Glostrup, Denmark) and visualization by the ECL method (Amersham Pharmacia Biotech).

Immunohistochemistry

Histopathology was evaluated from H&E-stained paraffin sections. For immunohistochemistry of paraformaldehyde-fixed paraffin sections, antigen retrieval, when applicable, was done with microwave treatment in 0.02 M sodium citrate for 15 min or trypsin digestion for 30 min followed by treatment with 3% hydrogen peroxide in methanol for 15 min. The primary antibodies used were monoclonal rat anti-mouse PECAM-1/CD31 (BD), goat anti-human VEGFR-3 (R&D Systems, Minneapolis, MN), affinity-purified polyclonal rabbit antikeratin 1, antikeratin 5, and antikeratin 10 (Covance), anti-Ki67 (Novocastra Laboratories Ltd., Newcastle upon Tyne, United Kingdom) as well as anti-α-smooth muscle actin (Sigma-Aldrich, St. Louis, MO). The proliferating cell nuclear antigen (PCNA) staining kit (Zymed Laboratories, South San Francisco, CA) and the apoptosis detection reagent (In Situ Cell Death Detection Kit, Roche Diagnostics GmbH, Mannheim, Germany) were used according to the manufacturer's protocol. Sections were incubated for 30 min with biotinylated rabbit anti-rat (Vector Laboratories, Burlingame, CA) or goat anti-rabbit antibodies (Vector Laboratories), followed by staining with the Vectastain Elite avidin-biotin complex (ABC)/HRP kit (Vector Laboratories) or a Tyramide Signal Amplification kit (TSA, NEN Life Sciences, Boston, MA). Staining was developed with 3-amino-9-ethyl carbazole (Sigma-Aldrich) as the chromophore. Negative staining controls were done by omitting the primary antibodies. Whole-mount staining of blood and lymphatic vessels and β-galactosidase staining of tissues was done as previously described (Rajantie *et al.*, 2001; Saaristo *et al.*, 2002). For staining of hematopoietic cells, the tissues were embedded in OCT compound (Tissue-Tek, Sakura Finetek Europe, Zoeterwoude, Netherlands) and snap-frozen. After sectioning, the slides were fixed in acetone and stained overnight with primary antibodies rat anti-mouse CD45 (BD Biosciences/PharMingen), rat anti-mouse Ly-6G (BD), rat anti-mouse F4–80 (Serotec, Oslo, Norway), rat anti-mouse B220 (BD) or rat anti-mouse CD3 (BD). The sections were incubated with secondary antibodies for 30 min and mounted with antifading medium containing DABCO (Sigma-Aldrich). Secondary antibodies with fluorochrome conjugates used were goat anti-rat Alexa[594] and donkey anti-rat Alexa[488] (Molecular Probes, Eugene, OR). Cell nuclei were visualized with the Hoechst fluorochrome (Sigma-Aldrich). Mast cells were quantified from toluidine blue–stained sections.

Cell Culture, Production of Retroviruses, and Infection of MMC-E Cells

All cells were grown in DMEM containing 4.5 g/l glucose, 10% fetal calf serum (FCS), glutamine, and antibiotics. Phoenix-Eco retrovirus packaging cells (a kind gift from Dr. G. Nolan) were transfected with 8 μg retroviral vector using Lipofectamine 2000 reagent (Invitrogen, Carlsbad, CA). Supernatants were harvested 40 h after transfection and filtered, and polybrene (Sigma-Aldrich) was added to a final concentration of 8 μg/ml. The MMC-E epithelial cells (Rapp *et al.*, 1979) were plated at 1.2×10^5 cells per well in a six-well plate. The next day, 2 ml of the harvested virus supernatants was added on the MMC-E cells. The cells were incubated for 10 min at 37°C after which the plates were centrifuged for 30 min at 2500 rpm (corresponding to $1150 \times g$) followed by a second incubation for 10 min at 37°C. The viruses were removed and replaced with normal growth medium. The following day, the cells were switched to selection medium containing 2.5 μg/ml 3′-(γ-amino-p-methoxyhydrocinnamamido)-3′-deoxy-N,N-dimethyladenosine (puromycin; Sigma-Aldrich). The cells were kept in the selection medium until analyzed by Western blotting and BrdU incorporation 7 days later.

BrdU Labeling and Immunofluorescence Staining of Cells

The cells were transferred to low serum (0.5% FCS) medium 12 h before the assay. The cells were then allowed to incorporate 20 μM 5-bromo-2-deoxyuridine (BrdU) for 2 h at +37°C followed by fixation in MetOH. DNA was denaturated by adding 2 M HCl for 60 min at +37°C and neutralized with 0.1 M borate buffer, pH 8.5. The proliferating cells were stained with monoclonal rat anti-BrdU (Abcam Ltd., Cambridge, United Kingdom) and goat anti-rat Alexa[488] (Molecular Probes) antibodies. The nuclei were visualized by Hoechst 33258 fluorochrome (Sigma-Aldrich) and the percentage of positive BrdU cells was counted. Statistical analyses were performed using the unpaired Student's t test. $p < 0.05$ was considered statistically significant.

Plasmids

The cDNAs coding for wild-type or kinase-deficient (K445R) human Bmx with a C-terminal hemagglutinin (HA) tag (Rajantie *et al.*, 2001) were cloned as *PmeI* fragments into *SnaBI* sites of the retroviral vector pBabepuro (Morganstern and Land, 1990).

Analysis of RNA

Total RNAs from skins of newborn mice were extracted using RNeasy kit (Qiagen GmbH, Hilden, Germany) and treated with DNAse I (Invitrogen). The murine genome U74Av2 microarray gene chips (Affymetrix UK Ltd., High Wycombe, United Kingdom) were hybridized with labeled RNA and analyzed according to the manufacturer's protocol as previously described (Petrova *et al.*, 2002). Reverse transcription was carried out from 1 μg of total RNA using the SuperScript II (Invitrogen) system, primed with oligo dT in a reaction volume of 10 μl. Amplification of the RT product was carried out with Dynazyme polymerase (Finnzymes) in a total volume of 50 μl under the following conditions: denaturation at 94°C for 30 s, annealing at 58°C for 30 s, and extension at 72°C for 60 s, 35 cycles. The primer pairs used were: IL-6, expected PCR product length 521 base pairs: 5′-AGTTGCCTTCTTGG-
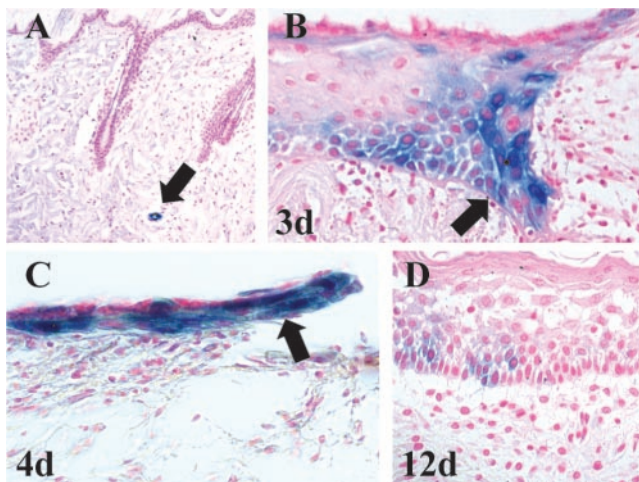
Figure 1. Bmx expression during wound healing analyzed in Bmx$^{LacZ/LacZ}$ mice. In normal skin β-galactosidase staining was seen only in arterial endothelium (A, arrow). In the healing wound, the proliferating and migrating basal keratinocytes and the leading edge of the migrating epithelium stain strongly for β-galactosidase (here days 3 (B) and 4 (C), arrows). Very few cells are stained in the healed epidermis (D; here day 12). Counterstaining is with nuclear red.

GACTGA-3′ and 5′-GCCACTCCTTCTGTGACTCC–3′; COX-2, 543 base pairs: 5′-TCCTCCTGGAACATGGACTC -3′ and 5′-TGATGGTGGCTGTTTT-GGTA -3′; CXCL-1, 274 base pairs: 5′-ACCCGCTCGCTTCTCTGT -3′ and 5′-TGGGGACACCTTTTAGCATC -3′; CXCL-5, 356 base pairs: 5′-GTTC-CAGCTCGCCATTCAT -3′ and 5′-TTGAACACTGGCCGTTCTTT -3′; E-selectin, 605 base pairs: 5′-GCAAAGCTGTCCAGTGTGAA -3′ and 5′-CGCA-GAAAGTGCAACTACCA -3′; MMP-3, 582 base pairs: 5′-CAGACTTGT-CCCGTTTCCAT -3′ and 5′-CCACCCTTGAGTCAACACCT -3′; BSSP, 525 base pairs: 5′-GGTCCTCATTGACCCACAGT -3′ and 5′-GGCTTCTCCTTT-GATCCACA -3′; β-actin, 573 base pairs: 5′-TGTTACCAACTGGGACGACA -3′ and 5′-AAGGAAGGCTGGAAAAGAGC -3′. After PCR amplification, 25 μl (for β-actin 10 μl) of the PCR products were separated in a 1.3% agarose gel and photographed.

RESULTS

Bmx Expression Is Induced in Epidermis during Wound Healing

We have previously shown that Bmx is expressed in arterial endothelial cells as well as in certain epithelial cells (Ekman *et al.*, 1997; Rajantie *et al.*, 2001). However, the function of Bmx in these cells is unknown because the Bmx knock-out (KO) mice did not show any obvious phenotype (Rajantie *et al.*, 2001). Histological analysis of the skin revealed no differences between the KO mice and wild-type (WT) mice (our unpublished results). To study a possible role for Bmx during wound healing, cutaneous punch-biopsy wounds were made in homozygous KO mice expressing the *LacZ* marker gene in the Bmx locus. Because no antibodies against murine Bmx were available that work in immunohistochemistry, Bmx expression was monitored by staining for β-galactosidase in skin samples taken at various time points during the healing. In nonwounded skin of the Bmx-KO mice, staining was seen only in the endothelium of arteries and arterioles of the dermis (Figure 1A, arrow), in accordance with our previously published results (Rajantie *et al.*, 2001). Surprisingly, however, analysis of the punch-biopsy wounds revealed that the *Bmx* gene was strongly up-regulated in the basal keratinocytes at the wound edge beginning on day 2–3 (Figure 1B, arrow). The expression of Bmx was subsequently seen during the whole reepithelialization phase in the mi-

grating and proliferating epidermal keratinocytes of the epidermal "leading edge" (Figure 1C, arrow). Bmx expression subsided immediately upon reepithelialization between days 5–7. In accordance, only weak Bmx expression was seen in a few cells of the thickened epidermis after wound closure (Figure 1D).

There was no difference in the kinetics of wound healing between the Bmx-KO mice and their WT littermates, neither did we see differences in the wound granulation tissue development including wound angiogenesis and the inflammatory response. No β-galactosidase staining was seen at any time point in the blood vessels of the granulation tissue (our unpublished results), indicating that Bmx expression is not involved in angiogenesis associated with skin wound healing. Neither was Bmx expression detected in the tumor vasculature of syngenic T241 fibrosarcomas growing subcutaneously in the Bmx-KO mice (our unpublished results). From these studies, we conclude that Bmx does not have a central role in wound healing angiogenesis or tumor angiogenesis, but that it is strongly up-regulated in the migrating epithelial cells in cutaneous wounds.

The K14-Bmx Mice Display Epidermal Hyperproliferation

To study the role of Bmx in epidermal cells of the skin, we generated mice overexpressing Bmx under the control of the keratin 14 promoter. This promoter directs transgene expression preferentially to the basal skin keratinocytes and the outer root sheaths of hair follicles (Vassar *et al.*, 1989). Several transgenic (TG) founder lines were produced and analyzed for the expression of the Bmx mRNA and protein (Figure 2A shows TG protein expression in one founder line.). For further analysis of the mice, three founder lines with high expression levels were used. All three gave similar results in the analyses.

The TG mice expressing Bmx in the basal keratinocytes were fertile and had a normal life span. However, in comparison with the WT littermates, the TG mice were smaller, had poorly developed hair, and typically absence of whiskers (Figure 2B, arrowhead, and our unpublished results). In histological analysis of newborn mice, the TG pups showed a markedly thickened epidermis as well as increased dermal cellularity. Depending on the age of the mouse, the epidermis was found to be ~2–3-fold thicker when compared with WT littermates (Figure 2, C and D). In addition, the dermal blood vessels of the TG mice were more numerous and enlarged (Figure 2, C and D, arrowheads). Basal keratinocytes of adult TG mice showed hyperproliferation as determined by staining for the cell proliferation markers PCNA (Figure 2, E and F) and Ki67 (our unpublished results). In contrast, the number of apoptotic cells was not increased in the skin of the TG mice when compared with WT mouse skin (Figure 2, G and H).

The most prominent epidermal thickening was seen in the tail (Figure 2, I and J). Interestingly, the tail epidermis showed psoriform characteristics such as elongated dermal papillae containing blood capillaries (Figure 2I, arrowhead), rete ridge-like changes (Figure 2I, arrow), and in addition to hyperkeratosis, also parakeratosis (Figure 2I, the retained nuclei are marked with asterisk). As expected, the proliferating cells were highly increased in the epidermis of the TG mice when compared with the WT mice (Figure 2, K and L). No clear histological changes were seen in other known sites of K14 expression, including the tongue, the esophagus, the intestine, and the thymus.

To study the effects of Bmx on epithelial cell proliferation, MMC-E epithelial cells were infected with retroviral vectors containing Bmx, kinase-deficient Bmx (K445R), or control
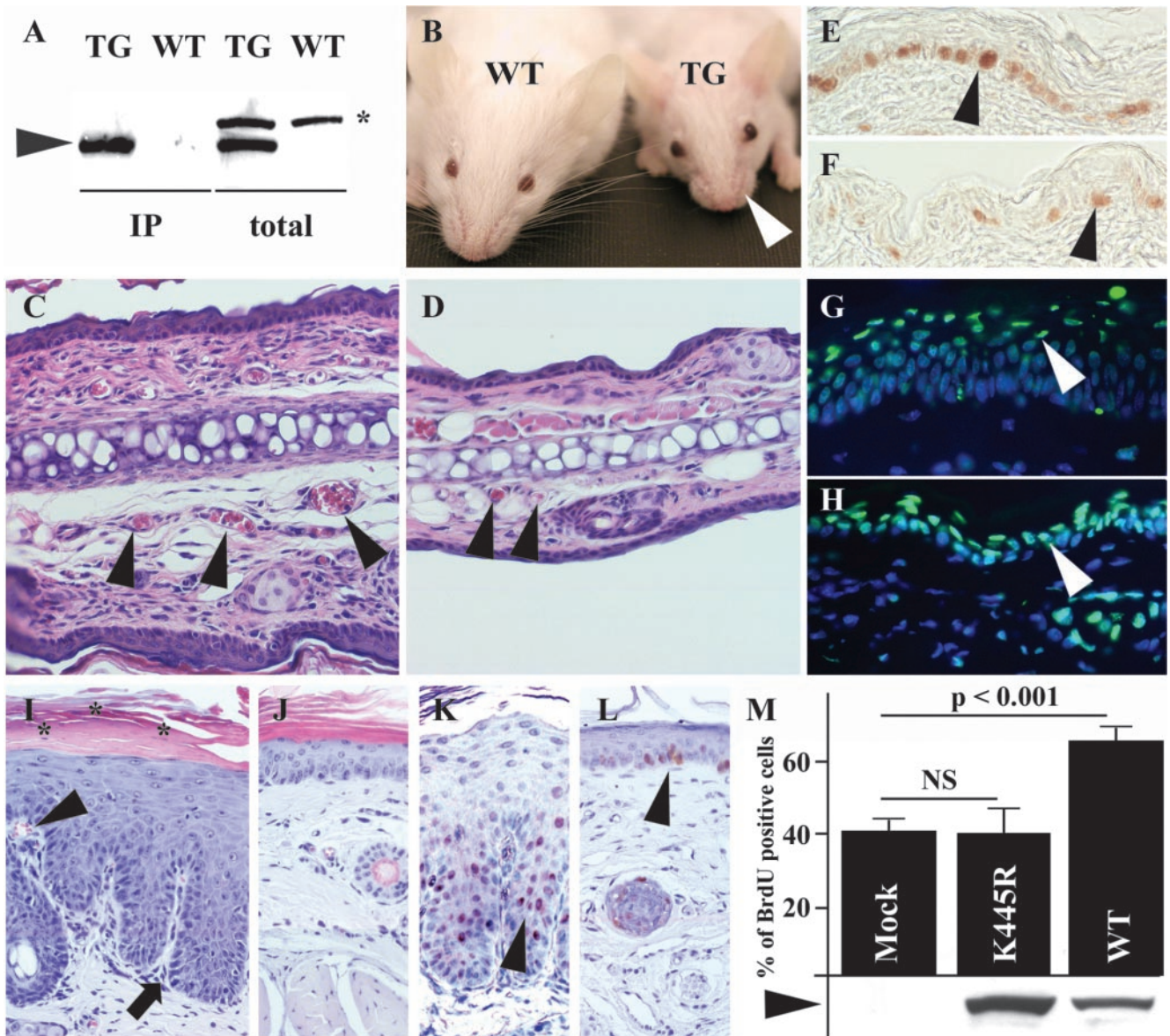
Figure 2. Comparison of K14-Bmx transgenic and control littermate mice. (A) Bmx expression (arrowhead) in TG mice analyzed by Western blotting of immunoprecipitates (IP) or total skin lysates (total). The asterisk indicates a nonspecific polypeptide. (B) Note the absent whiskers in TG mouse. H&E-stained cross sections from the ears of TG and WT mice (C and D). The arrowheads point to blood vessels in the cross sections. PCNA staining of the epidermis of back skin in TG (E) and WT mice (F). The arrowheads point to the proliferating basal cells. Sections of TG (G) and WT (H) ears stained for apoptotic cells (TUNEL; green, arrowheads) and cell nuclei (Hoechst; blue). Sections of tail skin of TG (I) and WT mice (J). Arrowhead shows the dermal papillae containing blood capillaries; arrow indicates the rete ridge-like changes in the skin; asterisk mark parakeratosis (retained cell nuclei in the horny layer of the epidermis). PCNA staining of tail sections of TG (K) and WT mice (L). Arrowheads indicate PCNA positive nuclei in the skin. (M) The percentage of BrdU-positive cells in MMC-E epithelial cells expressing mock vector (Mock), kinase-deficient Bmx (K445R) or Bmx (WT). Bars represent average counts from four separate infections and below are shown the relative protein amounts as detected by Western blotting. NS, not significant.

vector. Proliferation was quantified by measurement of BrdU incorporation into the cell nuclei after 5 days of growth in the selection medium. Bmx overexpression induced a >60% increase in epithelial cell proliferation in comparison to both mock vector (63.3% increase, $p < 0.001$) and kinase-deficient Bmx (65.3% increase, $p < 0.001$; Figure 2M).

Keratinocyte Differentiation and Dermal Inflammation

The TG mice had several layers of basal-like cells staining for keratin 5 (Figure 3A), a marker for basal keratinocytes. How-ever, orderly differentiation and keratinization appeared to occur in TG skin despite of the increased proliferation, as shown by staining of the top epidermal layers for markers of early and late keratinocyte differentiation, keratin 1 (Figure 3C) and keratin 10 (Figure 3E), respectively.

Immunofluorescence staining of the skin revealed an increased number of hematopoietic cells staining for the pan-leukocyte marker CD45 (Figure 3, G–H and I). When ear skin sections were stained for hematopoietic cell markers, a clear increase in the number of granulocytes and macro-
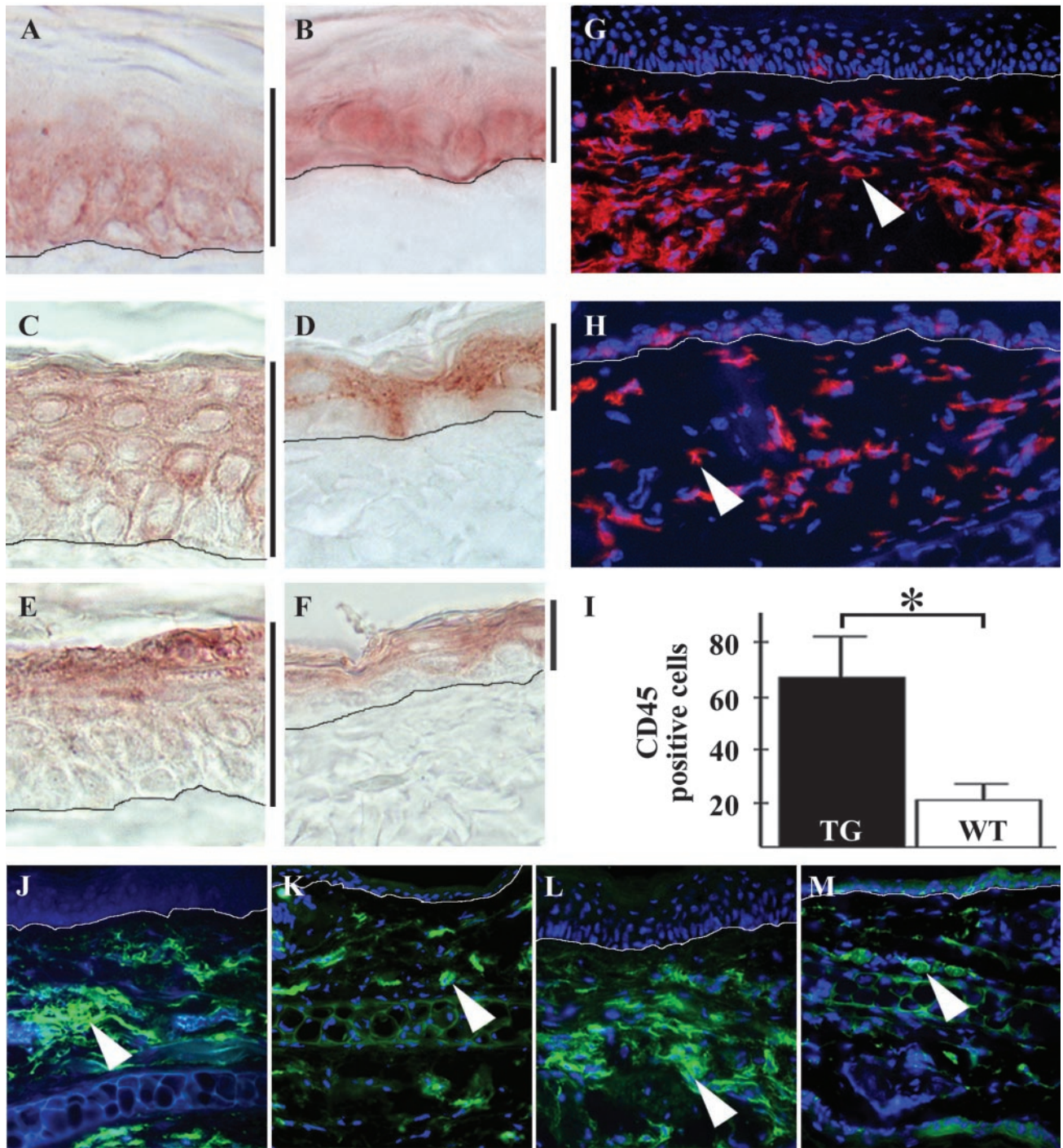
Figure 3. Immunohistochemical analysis of the K14-Bmx mouse skin. TG and WT skin stained for keratin 5 (A, TG; B, WT), keratin 1 (C, TG; D, WT) and keratin 10 (E, TG; F, WT). Vertical bars next to A–F denote epidermal thickness. Staining for CD45 in TG (G) and WT (H) ear cross sections, positive cells stain red (arrowheads). Cell nuclei stained with Hoechst; blue. Quantification of CD45-positive cells +SD (I). The asterisk indicates statistical significance (p < 0.001, Student's unpaired *t* test). Staining of the skin for the granulocytic marker Ly6G (J, TG; K, WT) and the macrophage marker F4/80 (L, TG; M, WT). The drawn perpendicular lines in A–H and J–M indicate the basement membrane of the epidermis in the skin cross sections. Cell nuclei are stained with Hoechst; blue.

phages could be seen in the TG mice when compared with the WT mice (Figure 3, J–M). The number of B- and T-lymphocytes, as well as toluidine blue–stained mast cells were comparable in TG and WT mice (our unpublished results).

Accelerated Wound Healing in the K14-Bmx Mice

Because endogenous *Bmx* was up-regulated in the proliferating and migrating keratinocytes during wound healing, we next studied the effect of Bmx overexpression on wound
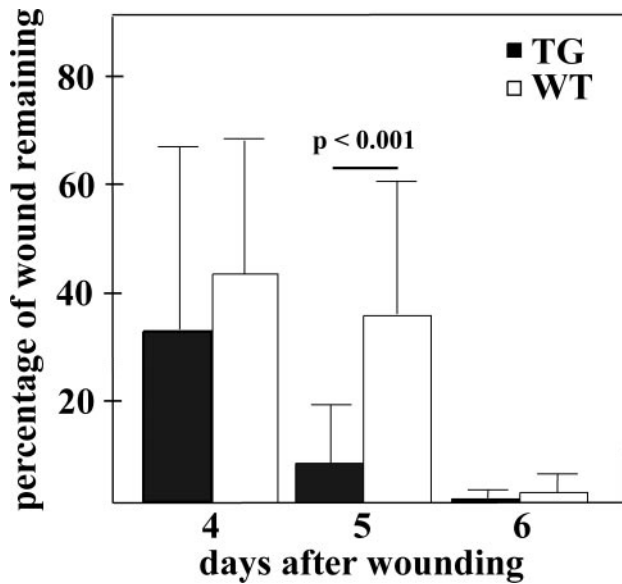
Figure 4. Wound healing in the K14-Bmx and control littermate mice. Bars represent the percentage of the remaining wound area +SD on days 4, 5, and 6 after wounding. All wounds had healed on day 7. Student's unpaired *t* test was used for statistical analysis.

Figure 5. Angiogenesis in the K14-Bmx mice. Whole-mount staining of TG and WT mouse ears for the vascular endothelial marker PECAM-1 (A–D) and for α-smooth muscle actin (SMA; E and F).

healing. The expression of K14 is up-regulated during skin wound healing (Werner *et al.,* 2000), making the K14-Bmx transgenic mouse model especially interesting for studies of the role of Bmx in the proliferating and migrating keratinocytes. On day 4 of the healing the wounds were still largely devoid of the epithelial layer and showed great variability in the healing, whereas on day 5 the reepithelialization of the wounds in the TG mice was significantly ($p < 0.001$) more advanced than in the WT mice (Figure 4). The K14 promoter is maximally up-regulated at day 5 of wound healing (Werner *et al.,* 2000), which correlates with the observed acceleration of wound healing in the K14-Bmx TG mice. On day 6 the wounds were nearly closed and complete reepithelialization was observed in both TG and WT mice by day 7.

K14-Bmx Mice Have an Abnormal Vasculature in the Skin

As is apparent from Figure 5, an increased number of large, tortuous blood vessels was observed in the dermis of the TG mice compared with WT mice. In several locations, the capillaries formed glomeruli-like structures staining for the blood endothelial marker PECAM-1/CD31 (Figure 5C, arrowhead). Some, but not all of the additional tortuous vessels were covered with α-smooth muscle actin (SMA)-positive cells (Figure 5E), indicating that maturation of the generated blood vessels to arteriae had also occurred in the skin. In contrast, the lymphatic vessels detected by staining for vascular endothelial growth factor receptor-3 appeared normal in number, size, and shape (our unpublished results).

Transcriptional Profiling Reveals Activation of Inflammatory Mediators in TG Skin

To analyze the molecular determinants of the transgenic skin phenotype, we compared the gene expression profiles of the skin from newborn TG and WT mice. Oligonucleotide microarrays, containing sequences from ~6000 known mouse ge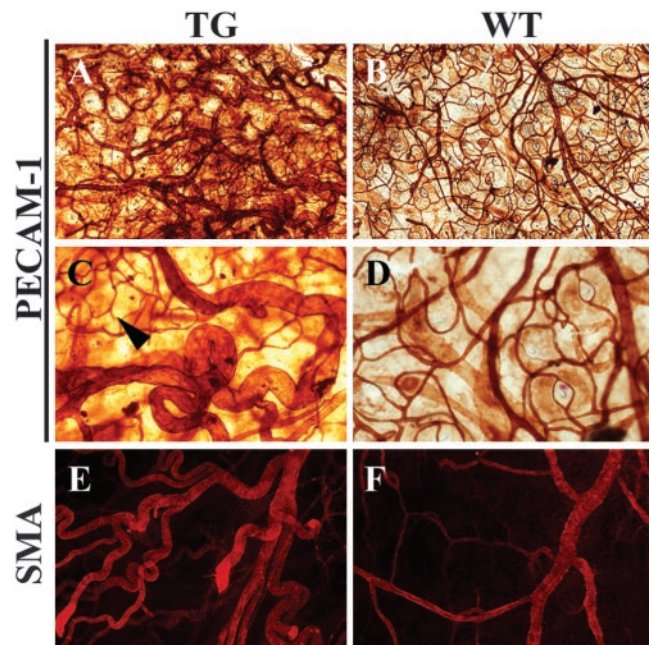nes and from 6000 expressed sequence tags (ESTs) were hybridized with labeled cRNA prepared from the back skin of the mice. In repeated experiments, 41 genes were found to be up-regulated and three genes down-regulated more than fourfold in the TG mice when compared with the WT mice (Table 1). The most interesting changes were confirmed by using RT-PCR (Figure 6) or Northern blotting analysis (our unpublished results). Several of the up-regulated genes are known to be involved in tissue inflammation, including the genes encoding endothelial selectin (E-selectin), cyclo-oxygenase-2 and the inflammatory and angiogenic mediator interleukin-6 as well as the angiogenic α-chemokines CXCL1 and CXCL5 (Epstein, 1998; Belperio *et al.,* 2000). The up-regulated genes included also stromelysin-1/ matrix metalloproteinase-3 (MMP-3), a proteinase with strong involvement in tumor development (Sternlicht *et al.,* 2000) and the serine protease BSSP, which is robustly induced in the skin by treatment with the tumor promoter phorbol ester 12-*O*-tetradecanoylphorbol-13-acetate (TPA; Breitenbach *et al.,* 2001). Furthermore, transcripts for keratin 6 and keratin 16, which are associated with epithelial hyperproliferation as well as for small proline-rich proteins (Sprr) associated with keratinocyte differentiation and epithelial barrier function (Tesfaigzi and Carlson, 1999; Chu and Weiss, 2002) were up-regulated.

DISCUSSION

Our present study shows that Bmx is strongly expressed in the proliferating and migrating epidermal keratinocytes during wound healing. Yet, there were no differences in skin histology or wound healing between the Bmx KO and WT mice, suggesting that other members of the Tec gene family may provide redundant functions in the epidermis. However, the epidermal Bmx transgene induced increased keratinocyte proliferation, inflammatory cell recruitment, and strong dermal angiogenesis as well as accelerated wound healing.

Table 1. Examples of genes with over 4-fold change of expression in TG vs. WT skin

Increased[a]

Growth factors and chemokines
  Interleukin-6*
  Growth-related oncogene alpha (CXCL1)*
  Endothelial-cell–derived neutrophil activating protein-78 (CXCL5)*
Adhesion molecules and proteolytic enzymes
  Endothelial Selectin (E-selectin)*
  A disintegrin and metalloproteinase-8 (ADAM-8)
  Matrix metalloproteinase-3 (MMP-3)*
  Brain-specific serine protease (BSSP)*
Signal transduction molecules and transcription factors
  Ets homologous factor (EHF)*
  Suppressor of cytokine signalling-3 (SOCS-3)
Inflammatory mediators
  Cyclo-oxygenase-2 (COX-2)*
  Myeloid-related protein 8 (MRP8)
  Myeloid-related protein 14 (MRP14)
  Glucocorticoid attenuated response gene 16 (GARG-16)
Epithelial structural proteins
  Small, proline-rich proteins (SPR)*
  Desmocollin-2
  Keratin 6
  Keratin 16

Decreased

Adhesion molecules and extracellular matrix proteins
  Fibulin-1
  Plexin B2

[a] The genes marked with an asterisk were verified by RT-PCR and/or Northern blotting.

The function and the signaling properties of Bmx have been mostly studied in cultured cells. Endogenous Bmx expression has been detected in cultured endothelial cells as well as in cultured prostate and breast carcinoma cells and
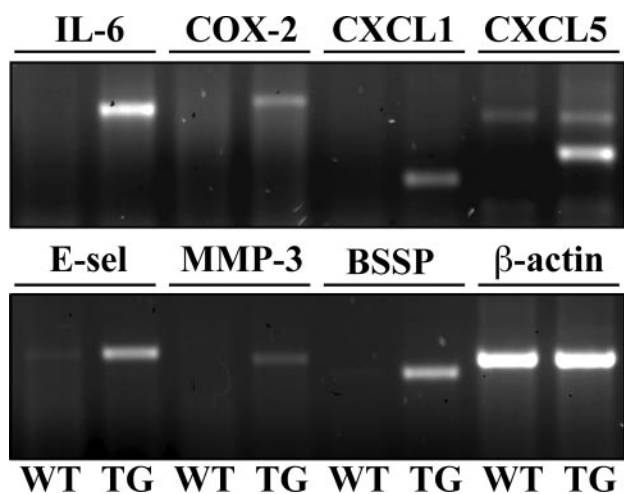
Figure 6. Analysis of differential gene expression in TG and WT skin by RT-PCR. RT-PCR of WT and TG newborn skin total RNA for several of the genes that were up-regulated in the TG skin in Affymetrix analysis. See text for details.

some studies have suggested Bmx association with the progression of prostate adenocarcinomas (Qiu *et al.*, 1998; Xue *et al.*, 1999; Chen *et al.*, 2001). In such cells Bmx was implicated in signaling for integrin- and tumor necrosis factor (TNF)-regulated cell migration and the expression of angiogenic factors (Chen *et al.*, 2001; Pan *et al.*, 2002; Zhang *et al.*, 2003). Bmx has also been implicated in the regulation of antiapoptotic pathways, cell proliferation, actin reorganization, and anchorage-independent cell growth and transformation (Xue *et al.*, 1999; Bagheri-Yarmand *et al.*, 2001; Chen *et al.*, 2001; Hamm-Alvarez *et al.*, 2001; Chau *et al.*, 2002). Taken together, these in vitro findings suggest a role for Bmx signaling in the regulation of cell migration and interestingly, also in tumor progression. However, such predictions have previously not been tested in vivo.

The K14-Bmx TG mice are the first model to address the above questions about Bmx function in vivo. The results obtained from the TG mice support the view that Bmx function is associated with epithelial cell proliferation and migration. The TG mice showed epidermal hyperproliferation with no changes in the rate of cellular apoptosis, resulting in a greatly thickened epidermis. Overexpression of Bmx resulted in acceleration of the wound closure by approximately one day. The observed kinetics of the Bmx effect may be explained by the fact that the K14 promoter is up-regulated beginning on days 2–3 after wounding and reaching a maximal sixfold induction on day 5 (Werner *et al.*, 2000). The proliferation-inducing effect of Bmx could be shown also in epithelial cells in culture. Bmx has been shown to mediate integrin signaling and cell migration in culture through binding of the Bmx PH domain to the FERM domain of FAK, resulting in Bmx activation (Chen *et al.*, 2001). FAK is thought to signal for cell migration via the docking protein p130Cas, which is a direct substrate for the Bmx tyrosine kinase (Abassi *et al.*, 2003). Thus the accelerated wound healing may be related to both increased keratinocyte proliferation and migration.

We also show that Bmx tyrosine kinase overexpression can trigger skin inflammation seen as the recruitment of leukocytes to the skin. This was accompanied by strong angiogenesis in the dermis with an increased number of large tortuous vessels in the TG mice when compared with WT littermate mice. Microarray analysis showed the upregulation of transcripts for several cytokines, chemokines, and other factors involved in the recruitment of inflammatory cells. We examined the possibility that the angiogenic effect is mediated by up-regulation of vascular endothelial growth factor (VEGF) because Bmx was recently shown to induce epithelial and endothelial cell proliferation by upregulating VEGF expression (Chau *et al.*, 2002). Because VEGF is a known activator of Bmx (Rajantie *et al.*, 2001), these results suggest a functional Bmx-VEGF autoregulatory loop (Rajantie *et al.*, 2001; Chau *et al.*, 2002). In addition, recent data have shown that Bmx is associated with TNF-mediated VEGFR-2 activation (Zhang *et al.*, 2003). However, despite the strong angiogenesis observed in the K14-Bmx TG skin, we did not detect increased levels of VEGF mRNA or protein in the skin. Angiogenesis observed in our model may thus be induced via angiogenic factors distinct from VEGF. For example, the angiogenesis could be directly stimulated by the angiogenic cytokines and growth factors that were overexpressed in the transgenic skin. On the other hand, the recruited inflammatory cells and their secreted cytokines could have a major role in triggering the vascular changes.

Taken together, the present data provide the first demonstration of Bmx function in vivo and the first phenotype

reported for a Tec family tyrosine kinase in normal mice. The Bmx TG mice now serve as an in vivo model for analysis of the effect of Bmx on the molecular mechanisms of epithelial cell proliferation and migration. These mice will also allow us to assess the function of Bmx in the progression of epithelial tumors, including possible effects on tumor angiogenesis.

ACKNOWLEDGMENTS

REFERENCES

Abassi, Y.A., Rehn, M., Ekman, N., Alitalo, K., and Vuori, K. (2003). p130Cas couples the tyrosine kinase Bmx/Etk with regulation of the actin cytoskeleton and cell migration. J. Biol. Chem. 278, 35636–35643.

Bagheri-Yarmand, R., Mandal, M., Taludker, A.H., Wang, R.A., Vadlamudi, R.K., Kung, H.J., and Kumar, R. (2001). Etk/Bmx tyrosine kinase activates Pak1 and regulates tumorigenicity of breast cancer cells. J. Biol. Chem. 276, 29403–29409.

Belperio, J.A., Keane, M.P., Arenberg, D.A., Addison, C.L., Ehlert, J.E., Burdick, M.D., and Strieter, R.M. (2000). CXC chemokines in angiogenesis. J. Leukoc. Biol. 68, 1–8.

Breitenbach, U., Tuckermann, J.P., Bebhardt, C., Richter, K.H., Furstenberger, G., Christofori, G., and Angel, P. (2001). Keratinocyte-specific onset of serine protease BSSP expression in experimental carcinogenesis. J. Invest. Dermatol. 117, 634–640.

Chau, C.H., Chen, K.Y., Deng, H.T., Kim, K.J., Hosoya, K., Terasaki, T., Shih, H.M., and Ann, D.K. (2002). Coordinating Etk/Bmx activation and VEGF upregulation to promote cell survival and proliferation. Oncogene 21, 8817–8829.

Chen, R., Kim, O., Li, M., Xiong, X., Guan, J.L., Kung, H.J., Chen, H., Shimizu, Y., and Qiu, Y. (2001). Regulation of the PH-domain-containing tyrosine kinase Etk by focal adhesion kinase through the FERM domain. Nat. Cell Biol. 3, 439–444.

Chu, P.G., and Weiss, L.M. (2002). Keratin expression in human tissues and neoplasms. Histopathology 40, 403–439.

Ekman, N., Arighi, E., Rajantie, I., Saharinen, P., Ristimaki, A., Silvennoinen, O., and Alitalo, K. (2000). The Bmx tyrosine kinase is activated by IL-3 and G-CSF in a PI-3K dependent manner. Oncogene 19, 4151–4158.

Ekman, N., Lymboussaki, A., Vastrik, I., Sarvas, K., Kaipainen, A., and Alitalo, K. (1997). Bmx tyrosine kinase is specifically expressed in the endocardium and the endothelium of large arteries. Circulation 96, 1729–1732.

Ellmeier, W., Jung, S., Sunshine, M.J., Hatam, F., Xu, Y., Baltimore, D., Mano, H., and Littman, D.R. (2000). Severe B cell deficiency in mice lacking the tec kinase family members Tec and Btk. J. Exp. med. 192, 1611–1624.

Epstein, F.H. (1998). Chemokines—chemotactic cytokines that mediate inflammation. New Engl. J. Med. 338, 436–445.

Fruman, D.A., Satterthwaite, A.B., and Witte, O.N. (2000). Xid-like phenotypes: a B cell signalosome takes shape. Immunity 13, 1–3.

Gutierrez, L.S., Schulman, A., Brito-Robinson, T., Noria, F., Ploplis, V.A., and Castellino, F.J. (2000). Tumor development is retarded in mice lacking the gene for urokinase-type plasminogen activator or its inhibitor, plasminogen activator inhibitor-1. Cancer Res. 60, 5839–5847.

Hamm-Alvarez, S.F., Chang, A., Wang, Y., Jerdeva, G., Lin, H.H., Kim, K.J., and Ann, D.K. (2001). Etk/Bmx activation modulates barrier function in epithelial cells. Am. J. Physiol. Cell Physiol. 280, C1657–C1668.

Honda, H., Mano, H., Katsuki, M., Yazaki, Y., and Hirai, H. (1995). Increased tyrosine-phophorylation of 55KDa proteins in beta-actin/Tec transgenic mice. Biochem. Biophys. Res. Commun. 206, 287–293.

Kaukonen, J., Lahtinen, I., Laine, S., Alitalo, K., and Palotie, A. (1996). BMX tyrosine kinase gene is expressed in granulocytes and myeloid leukaemias. Br. J. Haematol. 94, 455–460.

Liao, X.C., and Littman, D.R. (1995). Altered T cell receptor signaling and disrupted T cell development in mice lacking Itk. Immunity 3, 757–769.

Mano, H. (1999). Tec family of protein-tyrosine kinases: an overview of their structure and function. Cytokine Growth Factor 10, 267–280.

Morganstern, J.P., and Land, H. (1990). Advanced mammalian gene transfer: high titer retroviral vectors with multiple drug selection markers and a complementary helper-free packaging cell line. Nucleic Acids Res. 18, 3587–3596.

Pan, S., An, P., Zhang, R., He, X.R., Yin, G.Y., and Min, W. (2002). Etk/Bmx as a tumor necrosis factor receptor type 2-specific kinase: role in endothelial cell migration and angiogenesis. Mol. Cell. Biol. 22, 7512–7523.

Petrova, T.V. et al. (2002). Lymphatic endothelial reprogramming of vascular endothelial cells by the Prox-1 homeobox transcription factor. EMBO J. 21, 4593–4599.

Qiu, Y., and Kung, H.J. (2000). Signaling network of the Btk family kinases. Oncogene 19, 5651–5661.

Qiu, Y., Robinson, D., Pretlow, T., and Kung, H. (1998). Etk/Bmx, a tyrosine kinase with pleckstrin-homology domain, is an effector of phosphatidylinositol 3′-kinase and is involved in interleukin 6-induced neuroendocrine differentiation of prostate cancer cells. Proc. Natl. Acad. Sci. USA 95, 3644–3649.

Rajantie, I., Ekman, N., Iljin, K., Arighi, E., Gunji, Y., Kaukonen, J., Palotie, A., Dewerchin, M., Carmeliet, P., and Alitalo, K. (2001). Bmx tyrosine kinase has a redundant function downstream of angiopoietin and vascular endothelial growth factor receptors in arterial endothelium. Mol. Cell. Biol. 21, 4647–4655.

Rapp, U.R., Keski-Oja, J., and Heine, U.I. (1979). Establishment and characterization of the epithelial mouse embryo cell line MMC-E. Cancer Res. 39, 4111–4118.

Robinson, D., He, F., Pretlow, T., and Kung, H.J. (1996). A tyrosine kinase profile of prostate carcinoma. Proc. Nat. Acad. Sci. USA 93, 5958–5962.

Saaristo, A. et al. (2002). Adenoviral VEGF-C overexpression induces blood vessel enlargement, tortuosity, and leakiness but no sprouting angiogenesis in the skin or mucous membranes. FASEB J. 16, 1041–1049.

Satterthwaite, A.B., and Witte, O.N. (2000). The role of Bruton's tyrosine kinase in B-cell development and function: a genetic perspective. Immunol. Rev. 175, 120–127.

Schaeffer, E.M. et al. (1999). Requirement for Tec kinases Rlk and Itk in T cell receptor signaling and immunity. Science 284, 638–641.

Smith, C.I., Islam, T.C., Mattsson, P.T., Mohamed, A.J., Nore, B.F., and Vihinen, M. (2001). The Tec family of cytoplasmic tyrosine kinases: mammalian Btk, Bmx, Itk, Tec, Txk and homologs in other species. Bioessays 23, 436–446.

Sommers, C.L., Rabin, R.L., Grinberg, A., Tsay, H.C., Farber, J., and Love, P.E. (1999). A role for the Tec family tyrosine kinase Txk in T cell activation and thymocyte selection. J. Exp. Med. 190, 1427–1438.

Sternlicht, M.D., Bissell, M.J., and Werb, Z. (2000). The matrix metalloproteinase stromelysin-1 acts as a natural mammary tumor promoter. Oncogene 19, 1102–1113.

Tamagnone, L. et al. (1994). BMX, a novel nonreceptor tyrosine kinase gene of the BTK/ITK/TEC/TXK family located in chromosome Xp22.2. Oncogene 9, 3683–3688.

Tesfaigzi, J., and Carlson, D.M. (1999). Expression, regulation, and function of the SPR family of proteins. A review. Cell. Biochem. Biophys. 30, 243–265.

Vassar, R., Rosenberg, M., Ross, S., Tyner, A., and Fuchs, E. (1989). Tissue-specific and differentiation-specific expression of a human K14 keratin gene in transgenic mice. Proc. Natl. Acad. Sci. USA 86, 1563–1567.

Weil, D., Power, M.A., Smith, S.I., and Li, C.L. (1997). Predominant expression of murine Bmx tyrosine kinase in the granulo-monocytic lineage. Blood 90, 4332–4340.

Werner, S., Werner, S., and Munz, B. (2000). Suppression of keratin 15 expression by transforming growth factor beta in vitro and by cutaneous injury in vivo. Exp. Cell Res. 254, 80–90.

Xue, L.Y., Qiu, Y., He, J., Kung, H.J., and Oleinick, N.L. (1999). Etk/Bmx, a PH-domain containing tyrosine kinase, protects prostate cancer cells from apoptosis induced by photodynamic therapy or thapsigargin. Oncogene 18, 3391–3398.

Zhang, R., Xu, Y., Ekman, N., Wu, Z., Wu, J., Alitalo, K., and Min, W. (2003). Etk/Bmx transactivates vascular endothelial growth factor 2 and recruits phosphatidylinositol 3-kinase to mediate the tumor necrosis factor-induced angiogenic pathway. J. Biol. Chem. 278, 51267–51276.